

Research Article: New Research | Cognition and Behavior

Working-Memory Replay Prioritizes Weakly Attended Events

WM replay prioritizes weakly attended events

Anna Jafarpour^{1,2}, Will Penny³, Gareth Barnes³, Robert T. Knight^{1,2} and Emrah Duzel^{4,5,6}

¹Department of Psychology, University of California, Tolman Hall #1650, Berkeley, California 94720, USA

²Helen Wills Neuroscience Institute, University of California, 175 Li Ka Shing Center, Berkeley, California 94720, USA

³Wellcome Trust Centre for Neuroimaging at University College London, 12 Queen Square, London, WC1N 3BG, United Kingdom

⁴Institute of Cognitive Neuroscience, Alexandra House, 17-19 Queen Square, London, WC1N 3AR, United Kingdom

⁵German Centre for Neurodegenerative Diseases (DZNE), Leipziger Straße 44, Haus 64, Magdeburg, 39120, Germany

⁶Institute of Cognitive Neurology and Dementia Research, Otto-Von-Guericke, University of Magdeburg, Leipziger Straße 44, Haus 64, Magdeburg, 39120, Germany

DOI: 10.1523/ENEURO.0171-17.2017

Received: 17 May 2017

Revised: 27 June 2017

Accepted: 1 July 2017

Published: 14 August 2017

Author contributions: A.J. and E.D. designed research; A.J. performed research; A.J., W.P., and G.B. contributed unpublished reagents/analytic tools; A.J. and W.P. analyzed data; A.J., R.K., and E.D. wrote the paper.

Funding: Wellcome Trust

Funding: McDonnell Foundation

Funding: HHS | NIH | National Institute of Neurological Disorders and Stroke (NINDS)
100000065
R3721135

Conflict of Interest: Authors declare no conflict of interest.

Wellcome Trust; McDonnell Foundation; HHS | NIH | National Institute of Neurological Disorders and Stroke (NINDS) [R3721135].

Correspondence should be addressed to Anna Jafarpour, 132 Barker Hall, Knightlab, UC Berkeley, CA 94720. E-mail: a.jafarpour@berkeley.edu

Cite as: eNeuro 2017; 10.1523/ENEURO.0171-17.2017

Alerts: Sign up at eneuro.org/alerts to receive customized email alerts when the fully formatted version of this article is published.

Accepted manuscripts are peer-reviewed but have not been through the copyediting, formatting, or proofreading process.

Copyright © 2017 Jafarpour et al.

This is an open-access article distributed under the terms of the Creative Commons Attribution 4.0 International license, which permits unrestricted use, distribution and reproduction in any medium provided that the original work is properly attributed.

1 **Title:** Working-memory replay prioritizes weakly attended events

2 Abbreviated title: WM replay prioritizes weakly attended events

3 **Author Affiliation:** Anna Jafarpour ^{1,2*}, Will Penny ³, Gareth Barnes ³, Robert T.
4 Knight ^{1,2}, Emrah Duzel ^{4,5,6}

5 1 Tolman Hall #1650, Department of Psychology, University of California,
6 Berkeley, California 94720, United States of America.

7 2 Helen Wills Neuroscience Institute, 175 Li Ka Shing Center, University of
8 California, Berkeley, California 94720, United States of America.

9 3 Wellcome Trust Centre for Neuroimaging at University College London, 12
10 Queen Square, London, WC1N 3BG, United Kingdom.

11 4 Institute of Cognitive Neuroscience, Alexandra House, 17-19 Queen Square,
12 London WC1N 3AR, United Kingdom.

13 5 German Centre for Neurodegenerative Diseases (DZNE), Leipziger Straße 44,
14 Haus 64, 39120 Magdeburg, Germany.

15 6 Institute of Cognitive Neurology and Dementia Research, Otto-von-Guericke,
16 University, Magdeburg, Leipziger Straße 44, Haus 64, 39120 Magdeburg,
17 Germany.

18

19 * **Correspondence to:** 132 Barker Hall, Knightlab, UC Berkeley, CA 94720.

20 a.jafarpour@berkeley.edu

21 **Conflict of Interest:** Authors declare no conflict of interest.

22 **Acknowledgments:** We would like to thank Dr. Aidan Horner for constructive

23 discussions. This project was supported by the Wellcome Trust, NINDS Grant

24 R3721135, the Nielsen Corporation and the McDonnell Foundation.

25

26 **Abstract:** One view of working memory posits that maintaining a series of events
27 requires their sequential and equal mnemonic replay. Another view is that the content of
28 working memory maintenance is prioritized by attention. We decoded the dynamics for
29 retaining a sequence of items using magnetoencephalography (MEG), wherein
30 participants encoded sequences of three stimuli depicting a face, a manufactured
31 object, or a natural item and maintained them in working memory for 5 seconds.
32 Memory for sequence position and stimulus details were probed at the end of the
33 maintenance period. Decoding of brain activity revealed that one of the three stimuli
34 dominated maintenance independent of its sequence position or category; and memory
35 was enhanced for the selectively replayed stimulus. Analysis of event-related responses
36 during the encoding of the sequence showed that the selectively replayed stimuli were
37 determined by the degree of attention at encoding. The selectively replayed stimuli had
38 the weakest initial encoding indexed by weaker visual attention signals at encoding.
39 These findings do not rule out sequential mnemonic replay, but reveal that attention
40 influences the content of working memory maintenance by prioritizing replay of weakly
41 encoded events. We propose that the prioritization of weakly encoded stimuli protects
42 them from interference during the maintenance period whereas the more strongly
43 encoded stimuli can be retrieved from long-term memory at the end of the delay period.

44

45 **Significance Statement:** Here we show how information of a sequence of events is
46 prioritized in the working-memory maintenance buffer in humans. Participants retained
47 three consecutive visual stimuli and we decoded the content of working-memory
48 maintenance using multivariate-pattern-classification and magnetoencephalography

49 (MEG). We observed that the least attended events during encoding dominated the
 50 content of working-memory during the immediately following offline retention. In
 51 essence, the brain selectively and intelligently amplifies the least encoded memory item
 52 to maximize recall fidelity, instead of equally rehearsing the whole sequence. Our
 53 findings shift the functional role of working-memory from a faculty that “works with
 54 memory” to one that “works for memory” by actively selecting which encoded items
 55 need to be enhanced in order to be remembered.

56 **Introduction**

57 Working-memory is conceptualized as a mechanism to actively maintain and
 58 manipulate information (Baddeley, 1992). It is considered to consist of multiple layers,
 59 including long-term memory and a maintenance buffer - also known as the focus of
 60 attention during maintenance (Oberauer, 2002; Baddeley, 2010) that interacts with long-
 61 term memory. Working-memory maintenance is associated with a reactivation of
 62 information in non-human primates (Woloszyn and Sheinberg, 2009; Lee et al., 2005;
 63 Miller et al., 1993) and in humans (Lepsien and Nobre, 2007; Harrison and Tong, 2009;
 64 Fuentemilla et al., 2010). Here we investigated the representational content of
 65 maintaining a sequence of multiple stimuli in working memory. To decode
 66 representational content we employed multivariate pattern analysis (MVPA) of
 67 magnetoencephalography (MEG) recordings (Jafarpour et al., 2013; Cichy et al., 2014).

68 We addressed two hypotheses. The first hypothesis was that stimuli are maintained in a
 69 circular and repetitive structure. This hypothesis was motivated by the temporal coding
 70 model of working-memory maintenance which proposes that the replay mechanism
 71 conserves the temporal order in which stimuli were encountered (Lisman, 2010; Jensen

et al., 2014). Thus, the sequence of 1-2-3 circularly rehearses as 1-2-3-1-2-3-1-2-3-etc.

Such a dynamic has been reported in the medial temporal lobe of rodents (Jensen and Lisman, 1996), and the non-human primate prefrontal cortex (Siegel et al., 2009).

Support for the temporal coding model also comes from a recent human MEG study (Heusser et al., 2016). In that study, fitting the temporal coding model to whole brain MEG data source localized evidence for the model in the human hippocampus (Heusser et al., 2016). However, the trial-by-trial activity of non-human primate's prefrontal cortex supports a dynamic coding model of working memory, rather than the temporal coding model (Lundqvist et al., 2016). The dynamic coding model suggests that items are maintained in an "activity silent state" and replay is guided by attention (Stokes, 2015; Myers et al., 2017). Attention at encoding could thus prioritize the content of working memory such that working memory maintenance is dominated by a selected stimulus rather than the full to-be-memorized sequence. For instance, it would be more resource-effective to prioritize the less privileged stimuli at encoding to be replayed in working-memory (Zokaei et al., 2014; Stokes, 2015; Rose et al., 2016).

Here we used the whole brain MEG data to decode the content of working-memory. Our experiment was a modified version of the Sternberg task, where a sequence of three visual stimuli had to be retained. Objects from three distinct visual categories (Faces, manufactured objects, and natural items) were presented successively (the stimulus-set contained samples of the same items from different perspectives; Fig. 1B) followed by a five-second delay period. After the delay a probe queried stimulus identity (detail test) and a second probe queried the sequence of the three items (first, second, or third – order test; Fig. 1).

95 Pattern classifiers were trained on categorical representations of visual stimuli in brief
96 time-bins (20 milliseconds; ms) during encoding (Carlson et al., 2013; Jafarpour et al.,
97 2014). The classifiers labelled the on-going signal during retention (R) and inter-trial-
98 interval (ITI) periods for control. According to the output of the classifiers (face, banana,
99 chair, or 'none' for no replay), a Markov chain matrix of transitions between replayed
100 stimuli or 'none' was constructed (Fig. 2). With three stimuli, we could test for the
101 direction of replay (i.e. 1-2-3 versus 3-2-1). A Markov chain matrix of transitions
102 quantified the directional replay of sequences. The probability of transition from state 1
103 to 2, 2 to 3, and 3 to 1 would be higher than the probability of transition from state 1 to
104 3, 3 to 2, and 2 to 1, if there is a forward replay and the reverse pattern would be
105 observed for backward replay.

106 A support vector machine algorithm was used for decoding the (pairwise) categorical
107 information at -20 to 500 ms from onset of the visual stimuli during encoding. Note that
108 the categorical representation and item-specific representation overlaps in our case,
109 because we only used one sample from a category in this study (Fig. 1B). We trained
110 the classifiers on the amplitude of the broadband event-related single-trial MEG signals
111 and tested using a cross-validation method during encoding. We applied the classifiers
112 with best performances to decoding during the maintenance interval. To determine the
113 degree of attention during encoding, we analyzed early event-related fields (ERFs) to
114 each stimulus.

115 The sequential mnemonic replay hypothesis would predict decoding sequence
116 information or at least an equal probability of decoding all three encoded stimuli during
117 maintenance. In contrast, an attentional prioritization account would predict that the

118 degree of stimulus replay during the maintenance period would be dependent on the
119 size of early ERFs at encoding.

120 **Materials and Methods**

121 **Participants**

122 16 right-handed healthy adults with normal or corrected vision participated in this
123 experiment (8 female; on average 24 years old ($SD=2$)). The MEG data of two
124 participants were not included in the analysis, as their MEG signal was too noisy and
125 rejected as artefacts (for details see below). All participants gave written informed
126 consent and were compensated them financially for their participation. The University of
127 London Research Ethics Committee for human-based research approved the study.

128 **Experimental design**

129 We used a combination of a delay-match-to-sample and Sternberg tasks. The
130 experiment consisted of six runs, and each run consisted of 27 trials. Participants had
131 an optional five-minutes-break between runs. Each trial contained a sequential
132 presentation of three stimuli, a retention period, and two probe tests. A trial started with
133 a fixation (inter-trials interval) period for 4 seconds. Then a random sequence of three
134 stimuli appeared sequentially for 0.5 seconds, with a 0.5 second gap between stimuli. A
135 5 second retention period followed the presentation of the third item. Finally, a probe
136 stimulus was presented to test for item memory (delay-match-to-sample), where
137 subjects were required to select 'same' if the exact stimulus (category and perspective)
138 was shown in the sequence and 'different' otherwise (the perspective was different).
139 Randomly, in half of the trials, the correct answer was 'same'. For the following

question, subjects were required to answer “1, 2 or 3” according to the position of the probe in the sequence (Fig. 1A).

The stimuli were images from three visual categories for which previous multivariate decoding research indicated distinct spatial cortical representations (Kriegeskorte et al., 2008): a face, a fruit, and a manufactured object (Fig. 1B). Images were from three different perspectives – front-on, 60 degrees to the left, and 60 degrees to the right - shown upright on a white background, extending approximately 6 degrees of a horizontal and vertical visual angle. (face images were downloaded from Faces stimulus images Tarrlab, Centre for the Neural Basis of Cognition and Department of Psychology, Carnegie Mellon University, <http://www.tarrlab.org/>). Subjects were familiarized with the stimuli outside the MEG scanner and they also performed the experiment with feedback outside the scanner to ensure that they understood the experiment properly. There was no feedback given during the experiment inside the MEG scanner. In 6 runs each with 27 trials (all together, there were 162 trials), we tested all possible sequential combinations of three stimuli. All the possible combinations of three stimuli are 162 sequences: 6 combinations of sequences of three categorical stimuli, and 3 perspectives of each stimulus category ($= 6 \times 3 \times 3 \times 3$). We presented the trials randomly and each trial was seen once.

MEG recordings and data pre-processing

MEG data were recorded with a 274 channel CTF Omega whole-head gradiometer system (VSM MedTech, Coquitlam, BC, Canada) with a 600Hz sampling rate with an online bandpass filter from 0.1 to 200 Hz. Head position inside the system was tracked via head localizer coils attached to the nasion and 1cm anterior to the left and right pre-

163 auricular points. Participants sat upright and the stimuli were back-projected onto a
164 screen 1m in front of them.

165 MEG data were pre-processed using SPM12b (Wellcome Trust Centre for
166 Neuroimaging, London, www.fil.ion.ucl.ac.uk/spm) package and analyzed using Matlab
167 R2009b software. We filtered out the mains noise (50 Hz) from continuous signal using
168 a fifth-order Butterworth filter. We cropped the MEG data during encoding to epochs
169 from -100 to 500 ms from the stimuli onset. We discarded any epoch with field
170 magnitudes greater than 1.5×10^{-11} tesla in any channel, because it contained artefacts.
171 Two subjects had too many trials with such artefacts and were removed from further
172 analysis.

173 **Decoding the category of visual stimuli during encoding**

174 A Support Vector Machine (SVM) with a linear Kernel (Vapnik, 2000)– implemented in
175 statistics Matlab - was used to classify the signal elicited by the onset of the visual
176 stimuli. 26 classifiers were adopted at -20 to 500 ms from stimulus-onset during
177 encoding. The signal's sampling rate was 600 Hz. The signal was windowed in time-
178 bins of 20 ms (13 time points in each time-bin), centered at -10, 10, 30, 50, 70, 90, 110,
179 130, 150, 170, 190, 210, 230, 250, 270, 290, 310, 330, 350, 370, 390, 410, 430, 450,
180 470, and 490 ms. The single-trial input to the SVM classifiers was the broad-band
181 amplitude at each time point and each channel ($13 \times 274 = 3562$ features) for every
182 stimulus. The features were normalized before training, and the scale was used to
183 normalize features in testing data. We used a two-tailed t-test with a threshold of 0.05
184 for the feature reduction.

185 We trained three pairwise classifiers to decode the stimulus-category at each time-bin
 186 during encoding, irrespective of presentation order or perspective: face versus banana
 187 (FvsB), face versus chair (FvsC), and banana versus chair (BvsC). We identified the
 188 time-bins with reliable category stimulus classification and trained the classifiers on 90%
 189 of randomly selected samples from each category and tested them on 10% left-out
 190 samples from each category (i.e. 10-folds cross-validation). We selected an equal
 191 number of trials from each category for training and testing.

192 We examined the classification performance at the group level. To test the accuracy of
 193 each classifier against chance (i.e., 50%) we used a one sample t-test with a correction
 194 for multiple comparisons (family-wise error; FWE) using random field theory (RFT)
 195 implemented in SPM (Kilner et al., 2005; Litvak et al., 2011). As is standard in
 196 neuroimaging, we made inferences using a cluster-level threshold. The RFT procedure
 197 adjusts the p-value statistics that are functions of the number of time points
 198 (classification repetition). Such adjustment is similar to a Bonferroni correction.
 199 However, Bonferroni correction is suitable for data sets that are independent at each
 200 repetition (or data point). Here the data of adjacent time points is not independent and
 201 RFT is more suitable for multiple comparison correction (Kilner et al., 2005; Jafarpour et
 202 al., 2014).

203 **Decoding the category of visual stimuli during delay periods**

204 The most accurate classifiers from encoding were used to decode the replay during
 205 maintenance (the delay period between encoding and testing) and during the inter-trial
 206 intervals (ITIs; Fig. 2). For the delay period, we restricted analysis to the 1000 – 4000
 207 ms after the offset of the last stimulus in the sequence (150 time-bins were tested) in

208 order to exclude the event related activity elicited by offset of the last stimulus. We
209 selected the 3000 ms before onset of the first stimulus in the sequence (again including
210 150 time-bins) for testing the ITIs.

211 The outputs of the three pairwise-classifiers were class labels (F, B, or C) and distance
212 between unknown activity and classification decision boundaries. We determined the
213 decoded labels according to these outputs in two steps. First, we selected the class
214 label (between three classifier outputs) which had the largest distance to decision
215 boundaries. Second, we used a threshold to identify unknown activities that were too
216 close to the classification boundaries. We rejected these decoded classes and labelled
217 them as none (N).

218 A threshold was used to reject a percentage of classification outputs during retention
219 period. For example, if the classifier performance was reliable in 80% of times, we
220 rejected 20% labels of the decoded time-bins during retention. We applied the same
221 conservative threshold on decoded output during ITI. Following those steps, four
222 possible labels resulted from the classifiers: F, B, C, or N (for none – rejected
223 classifications; Fig. 2).

224 Two parameters were studied to quantify the differences in the decoding during the
225 retention period and the ITI in a trial by trial level. The first parameter was the number of
226 consecutive time bins decoded as the same item (i.e. a decoding epoch). We compared
227 the length of decoded epoch between the retention and ITI. We trusted that the
228 decoded items were replayed only when the memory benefited from the decoding (see
229 the analysis on the effect of active maintenance on behavioral responses).

230 The second parameter was the dynamics of replay extracted by the Markov chain. We
231 treated the classifiers outcomes as a state and counted the number of visits to the
232 states and transitions among them during retention and the ITI. We then extracted the
233 probabilities of transitions for each subject and compared between retention and inter-
234 trial intervals at the group-level using two-sided Wilcoxon rank sum test.

235 The directionality of replay was tested using two-sided Wilcoxon rank sum test. We
236 performed the following comparisons:

- 237 1. Probability of forward replay with the probability of backward replay-
238 Assuming an independent probability of replay of each stimulus, the forward
239 replay was the multiple of probability of transitions from the first stimulus to
240 the second stimulus, from the second stimulus to the third stimulus, and from
241 the third stimulus to the first stimulus. Backward replay was the multiple of
242 probability of transitions from the third stimulus to the second stimulus, from
243 the second stimulus to the first stimulus and from the first stimulus to the third
244 stimuli.
- 245 2. Probability of transitions from the first stimulus to the second stimulus with
246 probability of transitions from the first stimulus to the third stimulus.
- 247 3. Probability of transitions from the second stimulus to the first stimulus with
248 probability of transitions from the second stimulus to the third stimulus.
- 249 4. Probability of transitions from the third stimulus to the first stimulus with
250 probability of transitions from the third stimulus to the second stimulus.

251 **Effect of active maintenance on behavioral responses**

252 We applied a linear mixed-effects model to evaluate the effect of length of
 253 predominantly replayed epoch on the behavioral performance and response time across
 254 subjects. In each trial and for each probe (in both detail and order tests), we took the
 255 number of consecutive time-bins that the probe was replayed as a fixed variable and the
 256 subject number as a random variable. The effect of replay on behavior was visualized
 257 by grouping the probes according to whether or not they replayed during retention
 258 period and if replayed, whether the replay epoch was long (>1100 ms, based on Fig. 4)
 259 or short. We grouped the hit rate and response time accordingly. We studied the
 260 normalized behavioral performances and effect of active maintenance on behavior in
 261 the group-level using ANOVA and paired samples t-test for post-hoc tests -
 262 implemented in IBM SPSS Statistics v23.

263 **Event-related field (ERF) predicting predominant replay**

264 We investigated whether ERFs during stimulus presentation predicted maintenance.
 265 During maintenance one stimulus was predominantly replayed. We grouped event-
 266 related responses according to its replay during retention period: if the stimulus was
 267 predominantly maintained during retention interval (PM) or not (non-PM). We studied
 268 the event related field using SPM12b and ERF signals were baseline corrected based
 269 on the averaged amplitude in the whole epoch, and low-pass filtered at 20 Hz.

270 The significant effects were then source localized separately (an early effect peaked at
 271 125ms and a later effect peaked at 278 ms). We cropped the signal to 50 to 200 ms
 272 epoch to localize the first effect (115 to 135 ms), and cropped the signal to 200 to 350
 273 ms epoch to localize the later effect (270 to 300 ms). ERFs were source localized using

274 8192 vertices over the cortical surface in MNI space, a Single Shell as a forward model,
275 and multivariate sparse priors (MSP) (Friston et al., 2008). The individuals source
276 localized activity was then examined in a group level statistical analysis (Henson et al.,
277 2007).

278 **Results**

279 **Pattern classifiers performance**

280 We calculated the accuracies of three pairwise classifiers by averaging the classification
281 accuracies over validation-folds and paired categories. The results indicated that all
282 classifiers performed better than chance level (50%) from about 100 ms to 500 ms after
283 onset of the stimuli (out of -10 ms to 490 ms tested time-bins). F vs C classification
284 performance was above chance from 90 ms post stimulus onset with the highest
285 performance of 80% at 170 ms ($t(13) = 14.76$, FWE-corrected $P < 0.001$). The
286 performance for the B vs C classifier was also significant from 90 ms, with the best
287 performance of 75% at 190 ms ($t(13) = 14.61$, FWE-corrected $P < 0.001$). F vs B
288 classification was significant from 110 ms, with 80% performance 170 ms ($t(13) = 12.35$,
289 FWE-corrected $P < 0.001$; Fig. 3).

290 **Replay of one stimulus category dominates during retention**

291 The 170 ms classifiers had the highest performance during encoding (the averaged
292 cross-validated accuracy, over all three pairwise classifiers, was 78%). Thus, we
293 selected the 170 ms classifiers for decoding within two time windows where
294 maintenance may occur: Retention (R) interval itself and Inter-trial-intervals for control
295 (ITI). Each period contained 151 time-bins. Overall, we decoded overall about 330,000
296 time-bins.

297 The distributions of assigned category labels to each time-bin were different during R
 298 and ITI (Fig. 4). During R, the decoded adjacent time-bins were most frequently from
 299 the same category (see Fig. 4A as an example from a representative subject). We refer
 300 to these adjacent time-bins with the same decoded categories a replay ‘epoch’ – it
 301 quantifies the length of time staying in the same state. The lengths of all epochs
 302 (multiple per a delay period) were then calculated and the histogram of epoch lengths
 303 during R and ITI were compared in the four length-bins: 20 to 140 ms, 160 to 400 ms,
 304 420 to 1100 ms, and 1200 to 3000ms (note that a unit time-bin was 20 ms). We
 305 observed shorter replay epochs during ITI than R (20-140ms: $P < 0.001$), and longer
 306 replay epochs during R than ITI (420-1100 ms: $P = 0.007$; 1200-3000ms: $P < 0.001$;
 307 Fig. 4B).

308 The analysis was repeated after introducing the null category ('N') for no replays. We
 309 introduced a threshold for rejecting the classifier outputs that were close to classification
 310 decision boundaries. We labelled those rejected classifier outputs as null. For
 311 measuring the threshold, we first extracted the probability distribution of the distance to
 312 the classification boundaries (d) obtained from the R and the ITI periods (Fig. 4C). The
 313 applied classifier was accurate 78% of the time. We then selected a conservative
 314 threshold ($d^* = 2.49$) to reject 22% of outputs of the classifiers decoding the patterns
 315 during the retention period that were closest to the classification boundaries (they were
 316 the 22% top most ambiguous). The same threshold rejected 94% of the decoded
 317 patterns during ITI period. We labelled these rejected time-bins as 'N' for null.

318 After applying the threshold, the overall number of replays of 170 ms representations (F,
 319 B, and C) was higher during R (5422, SD = 1061) than ITI (92, SD = 149, $P < 0.001$) –

and the number of Ns (rejected bins) was higher during ITI (12657, SD = 2961) than R (3058, SD = 1669, $P < 0.001$). Furthermore, the decoded epochs were longer during R than ITI (in all four length-bins: $P < 0.001$; Fig. 4D), meaning that the replayed stimuli persisted over a longer period during R. These results indicated that during the retention period one stimulus was predominantly maintained (PM). There was no significant interaction between stimulus category and order and the predominant stimuli ($F(4,52) = 0.603$, $P = 0.662$); and no main effects of order ($F(2,26) = 0.747$, $P = 0.484$) or stimulus category ($F(2,26) = 0.701$, $P = 0.505$; Fig. 4E). At a group-level, the length of replay epochs for the predominantly maintained category was shorter than 160 ms in 25% (SD = 11.2) of trials, between 160 to 400 ms in 18.7% (SD = 4.5) of trials, between 420 to 1100 ms in 15.1% (SD = 3.8) of trials, and larger than 1100 ms in 41.3% (SD = 14) of trials.

No evidence for replay in sequential order

The difference between the pattern of replay during R and ITI was also detectable from the probability of replay of each stimulus at time-bin $t+1$ given replay of a stimulus at time-bin t – i.e. 1-step discrete-time Markov chain transition matrix between replayed states. If at time t a stimulus replays, most probably at time $t+1$ the same stimulus will replay (averaged probability of transition was %56.32). Probabilities of transitions to the same state and from N to each of the stimuli states were higher during R than ITI, and the probabilities of transitions from any state to N were lower during R than ITI. There was no difference between forward and backward transitions (Fig. 5).

Enhanced memory recall for the dominantly replayed stimuli

We then examined the behavioral performance for replayed stimuli by fitting a linear mixed-effects model: length of (longest) consecutive replay of the probes in each trial as a fixed variable and the subject identity as a random variable. The results showed significant effects of length of replay on the performance for detail test (parameter estimate: 0.0001; $t(2232) = 2.578$, $P = 0.01$) and on response time for the detail test (parameter estimate: -0.63175; $t(2232) = -2.115$, $P = 0.0345$). The result was not significant for the performance of order test (parameter estimate: < 0.0001 ; $t(2232) = 0.47757$, $P = 0.633$) or the response time of the order test (parameter estimate: 0.39498; $t(2232) = 1.1955$, $P = 0.232$).

We considered how long the probe's longest replay epoch was during the preceding retention interval. We grouped the probes into three: those with no replay (detail test: 72.1 probes (SD = 9.9), order test: 73.6 probes (SD = 12.4)), short replay epoch (less than 1100 ms (first three bars in Fig. 4); detail test: 64.1 probes (SD = 16.8), order test: 64.4 probes (SD = 16.1)), and long replay epoch (more than 1100 ms (last bar in Fig. 4); detail test: 23.8 probes (SD = 9.7), order test: 21.9 probes (SD = 8.9)). We also tested the behavioral responses accordingly to how long the probe replayed during retention. The effect of length of replay epoch predicted accuracy in the detail test (the first test the subjects performed after the retention period; $F(2,26) = 4.98$, $P = 0.015$). The post-hoc test showed that the hit rate was higher for the probes with long replay epochs than those with short replay epochs ($t(13) = 2.78$, $P = 0.016$) or those not replayed ($t(13) = 2.85$, $P = 0.014$; Fig. 6). We did not find any effect of replay on detail test response time

($F(2,26) = 1.89$, $P = 0.17$), order test response time ($F(2,26) = 0.20$, $P = 0.82$), or order test accuracy ($F(2,26) = 0.12$, $P = 0.89$).

Event-related activity during encoding predicts Item replay

Event related magnetic fields (ERFs) during encoding were examined as a function of which item was predominantly maintained (PM) during the retention period. The ERFs were pre-processed exactly the same way as the signal for pattern classification analysis and low-pass filtered at 20 Hz. The results revealed that PM and non-PM stimuli during encoding evoked significantly different ERFs at right temporal channels (peaked at 125 ms, $F(2,26) = 44.14$, FWE-corrected $P < 0.001$) and left temporal channels (peaked at 115 ms, $F(2,26) = 39.25$, FWE-corrected $P < 0.001$; and later peaks at 453 ms, $F(2,26) = 23.06$, $P = 0.008$; Fig. 7A and 7B), as well as at middle frontal channels (peaked at 287 ms, $F(2,26) = 32.49$, FWE-corrected $P = 0.002$, Fig 7C and 7D). The early ERF component (peaking at 125 ms) was source localized to the occipital temporal and the medial temporal cortices in both left and right hemispheres (Fig. 7E). The difference was significant in left occipital ($F(1,13) = 36.51$, FWE-corrected $P = 0.027$; Fig. 7E). The later ERF component, which peaked at 287 ms, was source localized to three brain regions, one on the left inferior temporal cortex ($F(1,13) = 21.85$, FWE-corrected $P = 0.033$, Fig. 7F) and two on the right inferior temporal cortex ($F(1,13) = 20.44$, FWE-corrected $P = 0.036$; and $F(1,13) = 19.03$, FWE-corrected $P = 0.42$; Fig. 7F).

Discussion

Using MEG, we decoded the content working-memory while individuals maintained the sequence and the visual details of three distinct stimuli. Our results revealed that one of

the three stimuli dominated the content of working-memory. The predominantly maintained item benefited memory performance, akin to the behavioral effect of retaining an item on the focus of attention (Lepsien and Nobre, 2007; Lepsien et al., 2011; Gazzaley and Nobre, 2012; Tan et al., 2014). The item selected for preferential replay was not predicted by the identity or the sequence position (Fig. 4E). Instead, the predominantly maintained stimulus was selected based on the lowest amount attention related event-related field (ERF) amplitude during encoding (Fig. 7).

Our strict criterion for the existence of a sequential replay was the probability of sequential transitions in a discrete-time (1 step) Markov chain transition matrix (Fig. 5). Accordingly, we did not find directional replay, namely any differences between the forward replay (1, 2, and then 3) or backward replay (3, 2, and then 1) (Fig. 5). In addition to this strict criterion, we tested a direct prediction of the temporal coding model. The temporal coding model predicts that all three memoranda would be decoded with equal probability during maintenance. This criterion was also not fulfilled (Fig. 6). These null findings have to be interpreted with caution because the spatiotemporal resolution of our methodology may not be sensitive to sequential replay and direct intracranial recording may be required to provide further evidence for or against these models. Furthermore, sequential replay may be recruited with higher working memory load than what was used in the current study (Heusser et al., 2016).

We observed that one stimulus dominated during the retention (Fig. 4). The identity of this stimulus varied from trial to trial. As noted, the category or the order of sequence did not determine what stimulus would replay (Fig. 4E). Instead, it was the amplitude of the ERFs at 125 ms from stimuli onset during encoding that predicted what stimulus

409 would replay (Fig. 7). The early effect was source localized to left extrastriate cortex
410 (Fig. 7), and this spatio-temporal pattern corresponds closely to the well-known effect of
411 attention to a visual stimulus during encoding (Heinze et al., 1990; Luck et al., 1990;
412 Okazaki et al., 2008; Rutman et al., 2009). Attention to a visual stimulus elicits an
413 enhanced event-related component in the occipital cortices (Hopf et al., 2000).
414 Specifically, allocating attention to visual stimuli increases the magnitude of event-
415 related EEG and MEG amplitude at around 100ms after the onset of visual stimulus
416 relative to less attended stimuli (Hillyard and Anllo-Vento, 1998; Downing, 2000). Thus,
417 stimuli that dominated replay during the retention interval were those that had received
418 the least early attention allocation during encoding. This early reduced attention effect
419 on the weakest encoded event was followed by a reduced amplitude event-related
420 response at 287 ms that source localized to posterior inferior temporal regions. This
421 indicates that the diminished early visual attention was followed by weaker
422 representations in downstream visual areas.

423 Our findings are compatible with long-standing research on how attention can influence
424 the content of working memory. Multiple items in working-memory are not all in the
425 same representational state during retention due to attention allocation (Zokaei et al.,
426 2014; Myers et al., 2017). Rather, brain stimulation or experimental instructions to
427 maintain a prompted stimulus (i.e. retro-cue procedure) manipulates the content of
428 retention (Lewis-Peacock and Postle, 2012; Zokaei et al., 2014; Rose et al., 2016).
429 Retro-cuing shifts the prompted stimulus into “the focus of attention”. In our experiment,
430 we did not employ retro-cues or brain stimulation; instead, all three visual items were

431 task-relevant. This procedure allowed us to uncover an uninstructed prioritization of
432 working-memory content that was dependent on the degree of early attention.

433 Our observation that one item can dominate the maintenance period is compatible with
434 recent neurophysiological data from the prefrontal cortex (PFC) of non-human primates.
435 These effects of replay on behavior suggest that only the item in the focus of attention is
436 actively replayed in working memory, while the representation of other stimuli are in an
437 “active-silent” state (Sandberg et al., 2003; Stokes, 2015). The active-silent state is
438 proposed to be a form of synaptic level retention where single unit activity drops to
439 baseline levels after an initial firing burst (Mongillo et al., 2008; Stokes, 2015; Lundqvist
440 et al., 2016).

441 An intriguing question raised by our data is how the weakly encoded stimuli are
442 prioritized for maintenance. Since prioritization was independent of sequence position, it
443 could have only occurred after all three stimuli were encountered. A parsimonious
444 scenario is that maintenance prioritization occurs at the beginning of the delay period
445 (perhaps in the PFC,(Lundqvist et al., 2016)) and involves retrieval of information. One
446 possibility is that the prioritized stimulus required more search or retrieval effort during
447 the delay. Such a process could have been supported by prefrontal mechanisms
448 allowing monitoring (Barbey et al., 2013; Szczepanski and Knight, 2014) and inhibitory
449 control (Knight et al., 1999; Barceló et al., 2000; Aron et al., 2004) reducing interference
450 (LaRocque et al., 2014; Zokaei et al., 2014) from strongly encoded stimuli. This
451 potential mechanism would compensate for capacity limitations of working-memory
452 (Luck and Vogel, 1997; Awh et al., 2006; Bays and Husain, 2008; Bays et al., 2009),
453 and would be more resource-effective by prioritizing the less privileged stimuli at

454 encoding in the maintenance buffer. In essence, the subjects enhanced replay of poorly
455 attended stimuli to improve subsequent performance. Whether more strongly attended
456 (higher amplitude early ERFs) stimuli were encoded into and retrieved from long-term
457 memory or whether they were in an “active silent” state (Stokes, 2015; Lundqvist et al.,
458 2016) remains an open question. Another option is that items were sequentially
459 replayed but when the signal for the weakly attended item was amplified; this masked
460 decoding of other items.

461 In summary, we decoded the dynamic replay of the content of visual working-memory
462 with high temporal resolution using MEG. The results revealed that the representation of
463 visual categorical information of the least attended stimuli during encoding was
464 preferentially replayed during retention. These findings reveal that working-memory
465 maintenance intelligently prioritizes the weakest attended and encoded task-relevant
466 stimuli enhancing the fidelity of memory recall.

467

References

- Aron AR, Robbins TW, Poldrack RA (2004) Inhibition and the right inferior frontal cortex. *Trends in Cognitive Sciences* 8:170–177.
- Awh E, Vogel EK, Oh S-H (2006) Interactions between attention and working memory. *Neuroscience* 139:201–208.
- Baddeley A (1992) Working memory. *Science* 255:556–559.
- Baddeley A (2010) Working memory. *Curr Biol* 20:R136–R140.
- Barbey AK, Koenigs M, Grafman J (2013) Dorsolateral prefrontal contributions to human working memory. *Cortex* 49:1195–1205.
- Barceló F, Suwazono S, Knight RT (2000) Prefrontal modulation of visual processing in humans. *Nat Neurosci* 3:399–403.
- Bays PM, Catalao RFG, Husain M (2009) The precision of visual working memory is set by allocation of a shared resource. *J Vis* 9 Available at: <http://www.journalofvision.org/content/9/10/7> [Accessed September 22, 2013].
- Bays PM, Husain M (2008) Dynamic shifts of limited working memory resources in human vision. *Science* 321:851–854.
- Carlson T, Tovar DA, Alink A, Kriegeskorte N (2013) Representational dynamics of object vision: The first 1000 ms. *J Vis* 13:1.
- Cichy RM, Pantazis D, Oliva A (2014) Resolving human object recognition in space and time. *Nat Neurosci* 17:455–462.
- Downing PE (2000) Interactions Between Visual Working Memory and Selective Attention. *Psychological Science* 11:467–473.
- Friston K, Harrison L, Daunizeau J, Kiebel S, Phillips C, Trujillo-Barreto N, Henson R, Flandin G, Mattout J (2008) Multiple sparse priors for the M/EEG inverse problem. *Neuroimage* 39:1104–1120.
- Fuentemilla L, Penny WD, Cashdollar N, Bunzeck N, Düzel E (2010) Theta-coupled periodic replay in working memory. *Curr Biol* 20:606–612.
- Gazzaley A, Nobre AC (2012) Top-down modulation: bridging selective attention and working memory. *Trends in Cognitive Sciences* 16:129–135.
- Harrison SA, Tong F (2009) Decoding reveals the contents of visual working memory in early visual areas. *Nature* 458:632–635.
- Heinze HJ, Luck SJ, Mangun GR, Hillyard SA (1990) Visual event-related potentials index focused attention within bilateral stimulus arrays. I. Evidence for early selection. *Electroencephalography and Clinical Neurophysiology* 75:511–527.

- 502 Henson RN, Mattout J, Singh KD, Barnes GR, Hillebrand A, Friston K (2007) Population-level inferences
503 for distributed MEG source localization under multiple constraints: application to face-evoked
504 fields. *Neuroimage* 38:422–438.
- 505 Heusser AC, Poeppel D, Ezzyat Y, Davachi L (2016) Episodic sequence memory is supported by a theta-
506 gamma phase code. *Nat Neurosci* 19:1374–1380.
- 507 Hillyard SA, Anllo-Vento L (1998) Event-related brain potentials in the study of visual selective attention.
508 *PNAS* 95:781–787.
- 509 Hopf J-M, Luck SJ, Girelli M, Hagner T, Mangun GR, Scheich H, Heinze H-J (2000) Neural Sources of
510 Focused Attention in Visual Search. *Cereb Cortex* 10:1233–1241.
- 511 Jafarpour A, Barnes G, Fuentemilla L, Duzel E, Penny WD (2013) Population Level Inference for
512 Multivariate MEG Analysis. *PLoS ONE* 8:e71305.
- 513 Jafarpour A, Fuentemilla L, Horner AJ, Penny W, Duzel E (2014) Replay of Very Early Encoding
514 Representations during Recollection. *J Neurosci* 34:242–248.
- 515 Jensen O, Gips B, Bergmann TO, Bonnefond M (2014) Temporal coding organized by coupled alpha and
516 gamma oscillations prioritize visual processing. *Trends Neurosci*.
- 517 Jensen O, Lisman J (1996) Hippocampal CA3 region predicts memory sequences: accounting for the
518 phase precession of place cells. *Learning and Memory* 3:279–287.
- 519 Kilner JM, Kiebel SJ, Friston KJ (2005) Applications of random field theory to electrophysiology. *Neurosci*
520 *Lett* 374:174–178.
- 521 Knight RT, Richard Staines W, Swick D, Chao LL (1999) Prefrontal cortex regulates inhibition and
522 excitation in distributed neural networks. *Acta Psychologica* 101:159–178.
- 523 Kriegeskorte N, Mur M, Ruff DA, Kiani R, Bodurka J, Esteky H, Tanaka K, Bandettini PA (2008) Matching
524 categorical object representations in inferior temporal cortex of man and monkey. *Neuron*
525 60:1126–1141.
- 526 LaRocque JJ, Lewis-Peacock JA, Postle BR (2014) Multiple neural states of representation in short-term
527 memory? It's a matter of attention. *Front Hum Neurosci* 8 Available at:
528 <http://www.ncbi.nlm.nih.gov/pmc/articles/PMC3899521/> [Accessed October 1, 2014].
- 529 Lee H, Simpson GV, Logothetis NK, Rainer G (2005) Phase Locking of Single Neuron Activity to Theta
530 Oscillations during Working Memory in Monkey Extrastriate Visual Cortex. *Neuron* 45:147–156.
- 531 Lepsien J, Nobre AC (2007) Attentional Modulation of Object Representations in Working Memory.
532 *Cereb Cortex* 17:2072–2083.
- 533 Lepsien J, Thornton I, Nobre AC (2011) Modulation of working-memory maintenance by directed
534 attention. *Neuropsychologia* 49:1569–1577.

- 535 Lewis-Peacock JA, Postle BR (2012) Decoding the internal focus of attention. *Neuropsychologia* 50:470–
536 478.
- 537 Lisman J (2010) Working memory: the importance of theta and gamma oscillations. *Curr Biol* 20:R490–
538 R492.
- 539 Litvak V, Mattout J, Kiebel S, Phillips C, Henson R, Kilner J, Barnes G, Oostenveld R, Daunizeau J, Flandin
540 G, Penny W, Friston K (2011) EEG and MEG data analysis in SPM8. *Comput Intell Neurosci*
541 2011:852961.
- 542 Luck SJ, Heinze HJ, Mangun GR, Hillyard SA (1990) Visual event-related potentials index focused
543 attention within bilateral stimulus arrays. II. Functional dissociation of P1 and N1 components.
544 *Electroencephalography and Clinical Neurophysiology* 75:528–542.
- 545 Luck SJ, Vogel EK (1997) The capacity of visual working memory for features and conjunctions. *Nature*
546 390:279–281.
- 547 Lundqvist M, Rose J, Herman P, Brincat SL, Buschman TJ, Miller EK (2016) Gamma and Beta Bursts
548 Underlie Working Memory. *Neuron* 90:152–164.
- 549 Miller EK, Li L, Desimone R (1993) Activity of neurons in anterior inferior temporal cortex during a short-
550 term memory task. *J Neurosci* 13:1460–1478.
- 551 Mongillo G, Barak O, Tsodyks M (2008) Synaptic Theory of Working Memory. *Science* 319:1543–1546.
- 552 Myers NE, Stokes MG, Nobre AC (2017) Prioritizing Information during Working Memory: Beyond
553 Sustained Internal Attention. *Trends in Cognitive Sciences* Available at:
554 <http://www.sciencedirect.com/science/article/pii/S1364661317300530> [Accessed May 12,
555 2017].
- 556 Oberauer K (2002) Access to information in working memory: Exploring the focus of attention. *Journal of*
557 *Experimental Psychology: Learning, Memory, and Cognition* 28:411–421.
- 558 Okazaki Y, Abrahamyan A, Stevens CJ, Ioannides AA (2008) The timing of face selectivity and attentional
559 modulation in visual processing. *Neuroscience* 152:1130–1144.
- 560 Rose NS, LaRocque JJ, Riggall AC, Gosseries O, Starrett MJ, Meyering EE, Postle BR (2016) Reactivation of
561 latent working memories with transcranial magnetic stimulation. *Science* 354:1136–1139.
- 562 Rutman AM, Clapp WC, Chadick JZ, Gazzaley A (2009) Early Top–Down Control of Visual Processing
563 Predicts Working Memory Performance. *Journal of Cognitive Neuroscience* 22:1224–1234.
- 564 Sandberg A, Tegnér J, Lansner A (2003) A working memory model based on fast Hebbian learning.
565 *Network: Computation in Neural Systems* 14:789–802.
- 566 Siegel M, Warden MR, Miller EK (2009) Phase-dependent neuronal coding of objects in short-term
567 memory. *PNAS* 106:21341–21346.

- 568 Stokes MG (2015) “Activity-silent” working memory in prefrontal cortex: a dynamic coding framework.
569 Trends in Cognitive Sciences 19:394–405.
- 570 Szczepanski SM, Knight RT (2014) Insights into Human Behavior from Lesions to the Prefrontal Cortex.
571 Neuron 83:1002–1018.
- 572 Tan J, Zhao Y, Wu S, Wang L, Hitchman G, Tian X, Li M, Hu L, Chen A (2014) The temporal dynamics of
573 visual working memory guidance of selective attention. Front Behav Neurosci 8 Available at:
574 <http://www.ncbi.nlm.nih.gov/pmc/articles/PMC4176477/> [Accessed December 17, 2014].
- 575 Vapnik V (2000) The Nature of Statistical Learning Theory. Springer.
- 576 Woloszyn L, Sheinberg DL (2009) Neural Dynamics in Inferior Temporal Cortex during a Visual Working
577 Memory Task. J Neurosci 29:5494–5507.
- 578 Zokaei N, Manohar S, Husain M, Feredoes E (2014) Causal Evidence for a Privileged Working Memory
579 State in Early Visual Cortex. J Neurosci 34:158–162.
- 580
581
582
583
584
585
586
587
588
589
590
591
592
593
594
595
596
597
598
599
600
601
602
603
604
605
606
607
608

609 **Figure Legends**

610 **Figure 1. Working-memory experimental paradigm (A)** three stimuli were presented
611 sequentially, each for 0.5 second and with 0.5 second gap between them. There was a
612 5 second retention period after the presentation of the third stimulus and memory probe
613 tests. The memory probe tests entailed a “same” or “different” judgment and a temporal
614 order decision. A four second inter-trial interval preceded the next trial. The labels R (in
615 blue) and ITI (in red) show the retention and inter-trial interval periods. **(B)** The stimuli
616 used in this experiment: a banana (B), a face (F) and a chair (C) from three points of
617 view, 60 degrees to the left, front on, 60 degrees to the right.

618 **Figure 2. Schema of the multivariate pattern analysis using SVM (A)** The state of
619 neural activity during delay (retention or ITI) periods was decoded at each time-bin,
620 using three pair-wise classifiers. A conservative threshold of d^* (depicted in red) was
621 used to reject representations which were close to the boundary and categorize them as
622 ‘N’ (the shaded area). **(B)** is a schematic example of decoded states during a delay
623 period. And **(C)** is the discrete-time Markov chain model of state transition extracted
624 from the schematic sequence in **(B)**.

625 **Figure 3. Multivariate classification of stimulus-categories: Cross-validation**
626 **performance**, these plots show the mean classification performance of 3 pairwise
627 classifiers across the group – left: F vs B, middle: F vs C, and right: B vs C. X-axis is the
628 time from stimulus (0 ms) and the Y-axis is the classification performance in %. The
629 error-bars show SEM. The grey area indicates significant classification after correction
630 for multiple comparisons.

631 **Figure 4. Decoding maintained categories in the delay period, (A)** a representative
 632 example (from one subject) of decoded retention (R) and inter trial interval (ITI) before
 633 thresholding. X-axis is the decoded time-bins, and Y-axis is the trial numbers. **(B)** the
 634 histogram of length of replay epochs during Retention (in blue) and during ITI (in red)
 635 before threshold: the x-axis shows the epoch length. The upper plot is the averaged
 636 epoch length from 20 – 3000 ms, and the bottom plot is the bar-plot for bins of epoch
 637 lengths (20-140 ms, 160-400 ms, 420-1100 ms, and 1200-3000ms). Error-bars show
 638 SEM. X-axis is length of epoch of stimuli replay. **(C)** The probability distribution of
 639 distance from classification boundaries during retention (blue) and ITI (red). d^* shows
 640 the threshold for rejecting 22% of classification outputs during retention. This threshold
 641 rejected 94% of classification outputs during ITI. **(D)** The same histograms as **(B)** but
 642 after applying the threshold. **(E)** The bar plots show the percentage of trials where the
 643 stimuli from the selected category (left plot) or order in the sequence (right plot) was
 644 predominantly maintained. There was no significant effect of category or order of
 645 stimuli.

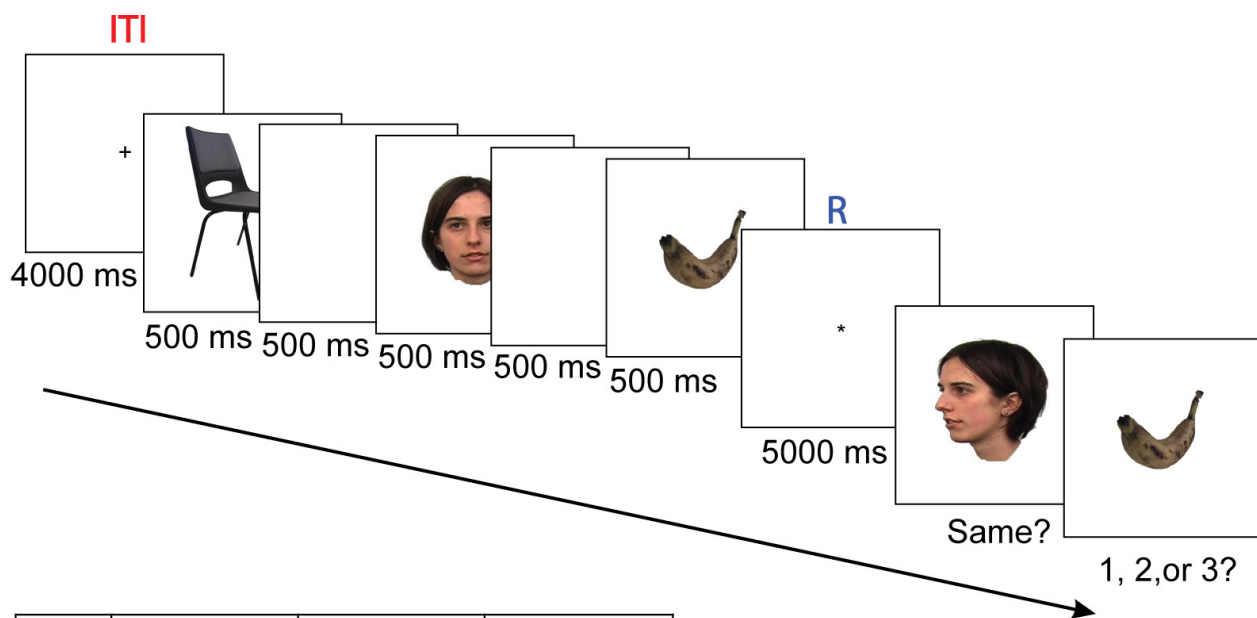
646 **Figure 5. Difference in averaged probability of state transition matrix** is reflected by
 647 the thickness of the arrows. The probabilities of all transitions were different between
 648 retention (R) periods and inter trial intervals (ITI). Red arrows show the transitions when
 649 the probabilities were more during ITI than R and blue arrows show the other way
 650 around. There was no difference between probabilities of forward (1-2-3) and backward
 651 (3-2-1) transitions.

652 **Figure 6. Effect of replay of 170 ms representation on WM performance (A)** for the
 653 detail test and **(B)** for the order test show the hit rate (%) with respect to whether the










stimuli were not replayed (none), replayed for a short duration (shorter than 1100 ms) or replayed for a long duration (longer than 1100 ms). Error-bars shows SEM. * $P < 0.05$.

Figure 7. ERFs during encoding differentiate between stimuli predominantly maintained (PM) in working memory and the non-PM stimuli. (A) The plots graph the F-statistics in channel by time topography. It focuses on the significant clusters at 0.125 s from the stimuli onset. The bottom plot shows channel by channel topography of the effect (x-axis is from left to right, and y-axis is from posterior to anterior). The upper plots are channel by time. The x-axis on the left plot shows channels from left to right and the x-axis on the right plot shows the channels from anterior to posterior. The peaks are highlighted with shapes in (A to D). (B) The top plot is for the effect peaked at 0.125 s ($P < 0.001$) in a left lateral channel, and the bottom plot is for the ERF effect at 0.453 s ($P = 0.008$) in a right lateral channel. The plots show the ERF effects in the peak of significant clusters, which are highlighted by shapes (A and B). The dash-lines show the timing of the effects. (C) The plots graph the F-statistics in channel by time (the same as A) focusing on the significant effect peaked at 0.287 s ($P = 0.002$). The effect is highlighted by a diamond shape in (C and D). (D) The plot shows the ERF effect at 0.287 s from the stimuli onset in a middle frontal channels. (E) The ERF effect at 0.125 s (A and B) was source localized in the bilateral occipital cortex. (F) The ERF effect at 0.287 s (C and D) was source localized in the posterior inferior temporal areas. (A to D) dotted line shows the onset of the stimuli at encoding.

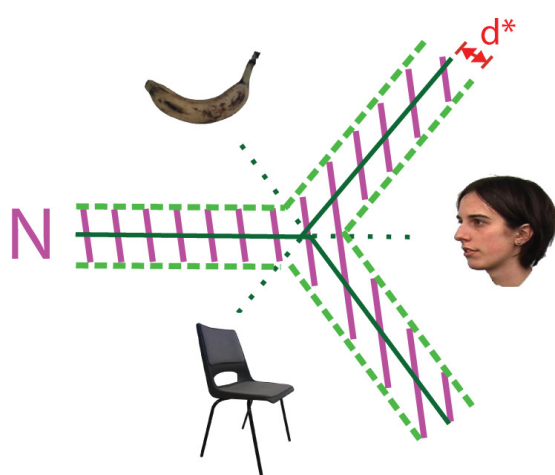
A



B

fruit (B)			
face (F)			
chair (C)			

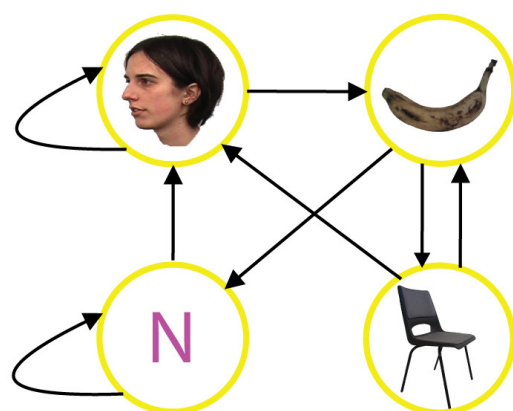
A

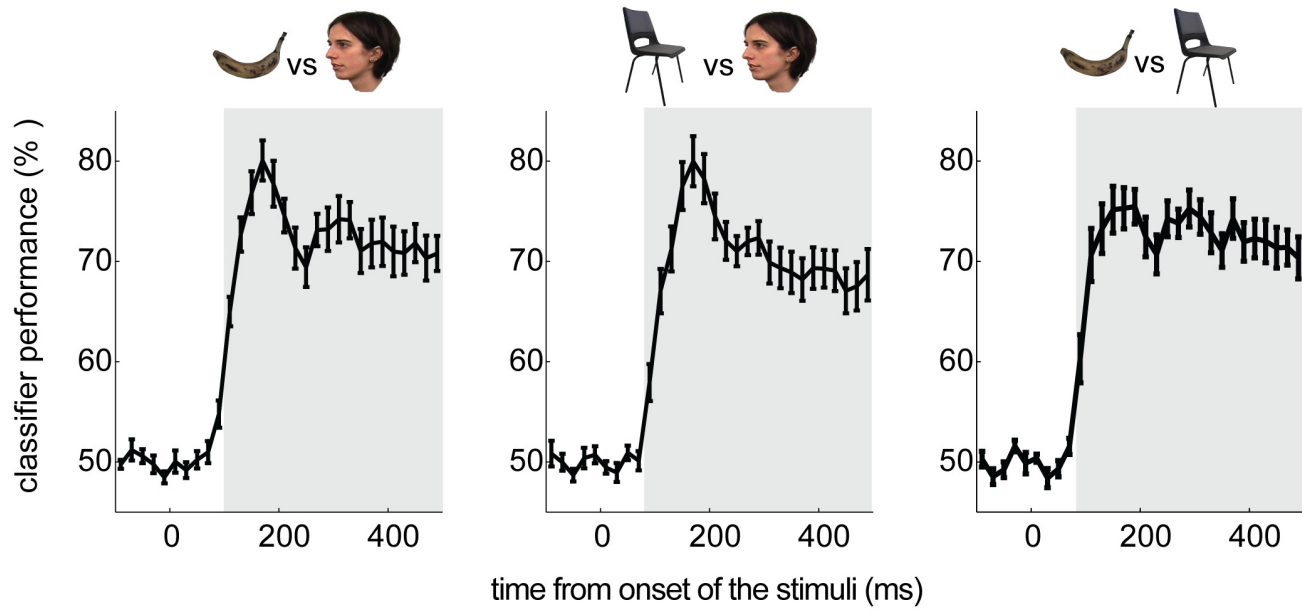


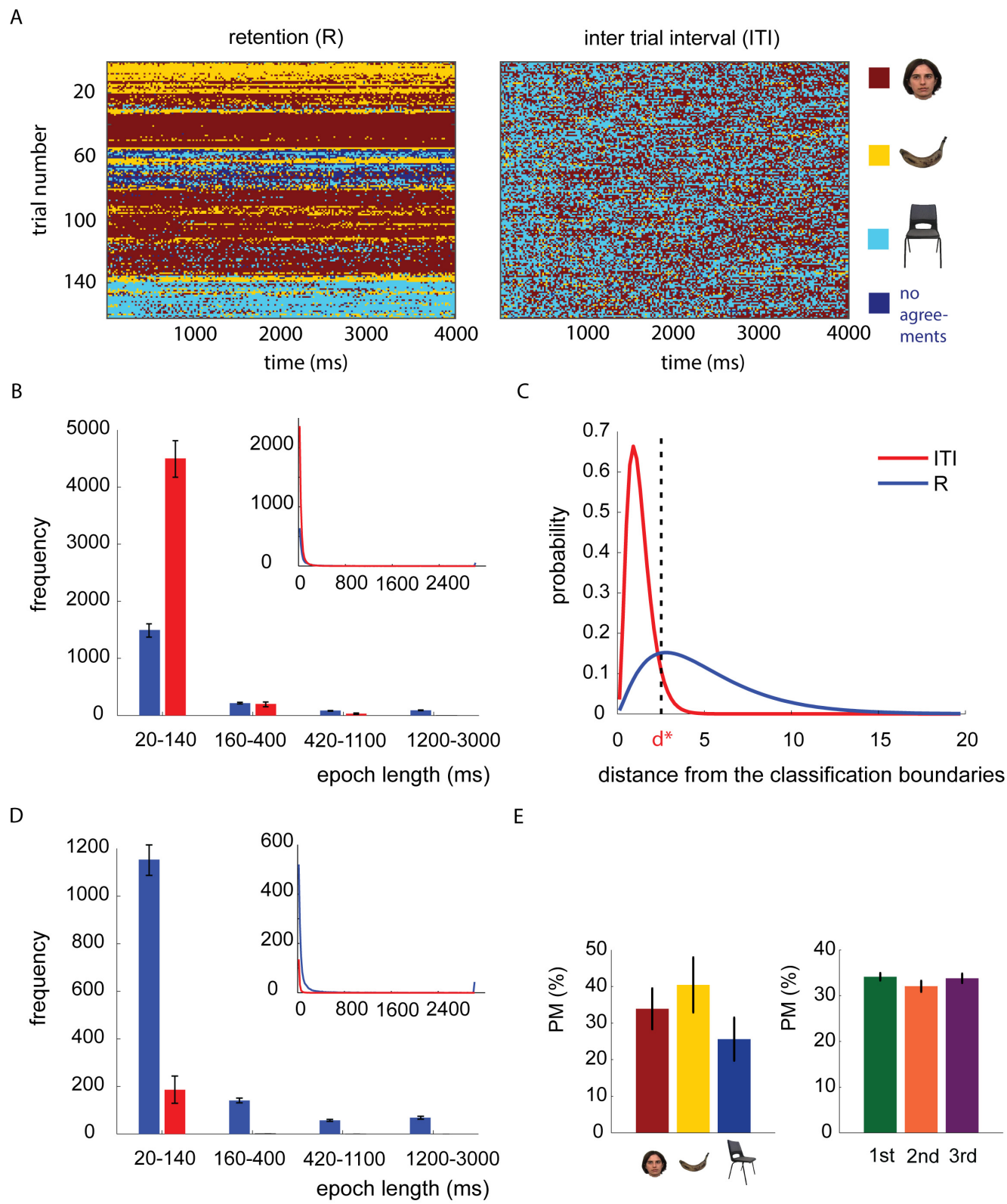
B

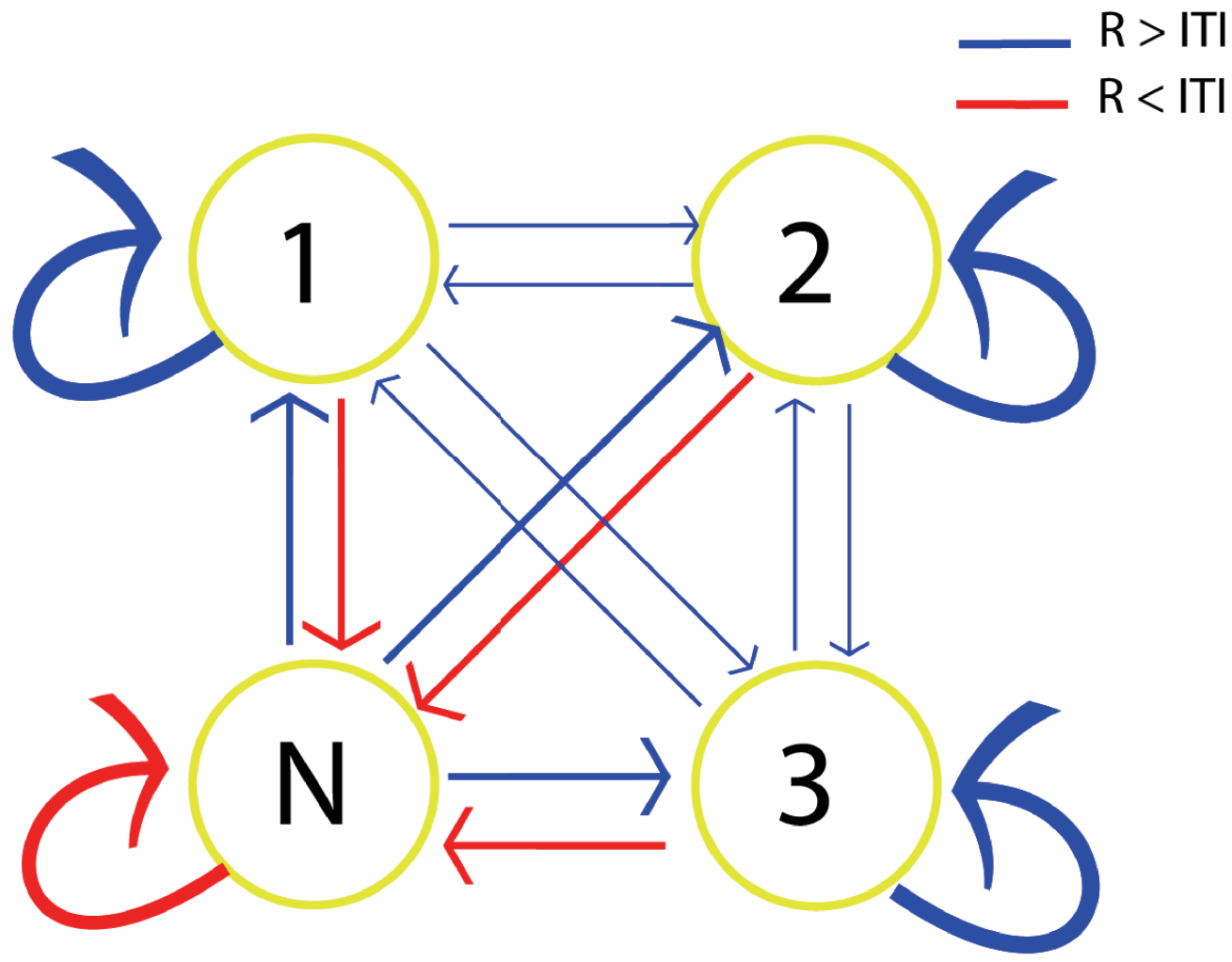


C

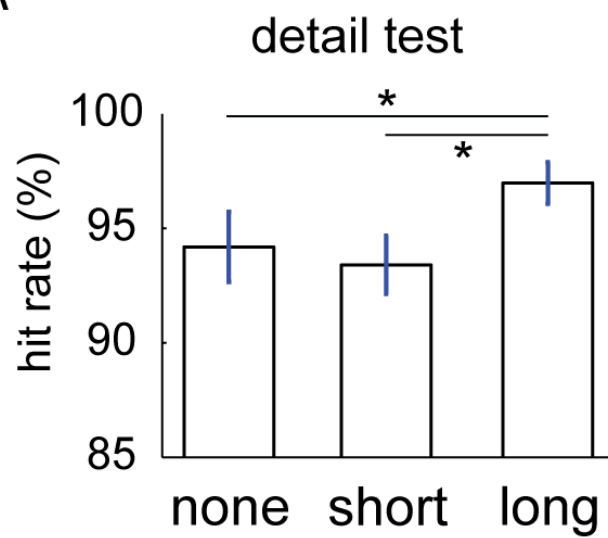








A



B

